Oral Peroxisome Proliferator–Activated Receptor-α Agonist Enhances Corneal Nerve Regeneration in Patients With Type 2 Diabetes

Calesta Hui Yi Teo,[1] Molly Tzu-Yu Lin,[2] Isabelle Xin Yu Lee,[2] Siew-Kwan Koh,[3] Lei Zhou,[3,4,5] Dylan Shaoying Goh,[6] Hyungwon Choi,[7] Hiromi Wai Ling Koh,[7] Amanda Yun Rui Lam,[8] Paik Shia Lim,[9] Jodhbir S. Mehta,[2,4,10,11] Jean-Paul Kovalik,[12] Thomas M. Coffman,[12] Hong Chang Tan,[8] and Yu-Chi Liu[2,4,10,11]

Diabetes 2023;72:932–946 | https://doi.org/10.2337/db22-0611

Diabetic corneal neuropathy (DCN) is a common complication of diabetes. However, there are very limited therapeutic options. We investigated the effects of a peroxisome proliferator–activated receptor-α (PPAR-α) agonist, fenofibrate, on 30 patients (60 eyes) with type 2 diabetes. On in vivo confocal microscopy evaluation, there was significant stimulation of corneal nerve regeneration and a reduction in nerve edema after 30 days of oral fenofibrate treatment, as evidenced by significant improvement in corneal nerve fiber density (CNFD) and corneal nerve fiber width, respectively. Corneal epithelial cell morphology also significantly improved in cell circularity. Upon clinical examination, fenofibrate significantly improved patients' neuropathic ocular surface status by increasing tear breakup time along with a reduction of corneal and conjunctival punctate keratopathy. Tear substance P (SP) concentrations significantly increased after treatment, suggesting an amelioration of ocular surface neuroinflammation. The changes in tear SP concentrations was also significantly associated with improvement in CNFD. Quantitative proteomic analysis demonstrated that fenofibrate significantly upregulated and modulated the neurotrophin signaling pathway and linolenic acid, cholesterol, and fat metabolism. Complement cascades, neutrophil reactions, and platelet activation were also significantly suppressed. Our results showed that fenofibrate could potentially be a novel treatment for patients with DCN.

Diabetic neuropathy is one of the most common microvascular complications of uncontrolled diabetes (1). Chronic hyperglycemia results in the accumulation of advanced glycation end products and the production of reactive oxygen species, both of which increases oxidative stress and inflammation to pericytes and endothelium of capillaries, thereby reducing microvascular supply to Schwan cells or neurons (2). Prolonged hyperglycemia also inhibits nerve growth factor (NGF) for neuronal health and myelin formation, leading to reduced nerve velocity (3). Collectively, these pathological processes damage neuronal tissues, leading to corneal denervation. The human cornea is densely innervated, and corneal nerves play an important neurotrophic role in maintaining ocular surface homeostasis, integrity, and functionality (4). Any degeneration or injury to the corneal nerves leads to a neuropathic

[1]Yong Loo Lin School of Medicine, National University of Singapore, Singapore
[2]Tissue Engineering and Cell Therapy Group, Singapore Eye Research Institute, Singapore
[3]Ocular Proteomic Group, Singapore Eye Research Institute, Singapore
[4]Ophthalmology and Visual Sciences Academic Clinical Program, Duke-NUS Medical School, Singapore
[5]Department of Ophthalmology, Yong Loo Lin School of Medicine, National University of Singapore, Singapore
[6]Department of Pharmacy, National University of Singapore, Singapore
[7]Department of Medicine, Yong Loo Lin School of Medicine, National University of Singapore, Singapore
[8]Department of Endocrinology, Singapore General Hospital, Singapore
[9]Department of Pharmacy, Singapore General Hospital, Singapore
[10]Cornea and Refractive Surgery Group, Singapore Eye Research Institute, Singapore
[11]Department of Cornea and External Eye Disease, Singapore National Eye Centre, Singapore
[12]Program in Cardiovascular and Metabolic Disorders, Duke-NUS Medical School, Singapore

Corresponding authors: Yu-Chi Liu, liuchiy@gmail.com, and Hong Chang Tan, tan.hong.chang@singhealth.com.sg

Received 8 July 2022 and accepted 15 November 2022

Clinical trial reg. no. NCT03869931, clinicaltrials.gov

This article contains supplementary material online at https://doi.org/10.2337/figshare.21583392.

See accompanying article, p. 838.

ocular surface, resulting in clinical presentations ranging from decreased corneal sensitivity to severe corneal perforation (5).

Diabetic corneal neuropathy (DCN) and its resultant diabetic keratopathy are underreported yet estimated to affect ∼47–64% of patients with diabetes (6). Despite the risk for corneal perforation and vision loss, the current mainstay management for diabetic keratopathy only focuses on symptomatic treatment, such as lubricants and prophylactic antibiotics. These treatments do not address the underlying pathophysiology (i.e., corneal neuropathy). Currently, recombinant NGF eye drops are the only U.S. Food and Drug Administration–approved drug for treating patients with neurotrophic keratopathy. However, this treatment course is costly and requires frequent topical application (7). In view of the significant disease incidence and limited treatment options, novel, effective, and affordable treatment is crucially needed.

Fenofibrate is a peroxisome proliferator–activated receptor-α (PPAR-α) agonist (8) known to regulate lipid and glucose metabolism (9). Through the activation of PPAR-α, this antilipidemic drug increases lipoprotein lipase activation, resulting in the rapid degradation of LDL and triglycerides (TGs) while increasing the synthesis of HDL cholesterol and stimulating the fatty acid oxidation pathway in tissues (10). We believe that these effects are helpful in protecting against nerve damage, as hypertriglyceridemia, hyperlipidemia, and decreased HDL cholesterol are known significant risk factors for the development of peripheral neuropathy (11).

Recently, two mouse studies (12,13) have shown that oral fenofibrate reduces neuroinflammation and improves axon regeneration of peripheral nerves via the activation of PPAR-α receptors. A separate study on diabetic mice demonstrated that fenofibrate treatment significantly prevented the development of diabetic peripheral neuropathy (DPN) by ameliorating neural, Schwann cell, and endothelial damage through the activation of the PPAR-α-AMPK-peroxisome proliferator–activated receptor γ coactivator 1α pathway (14). Additionally, the Fenofibrate Intervention and Event Lowering in Diabetes (FIELD) study reported that patients on fenofibrate had a significantly greater reversal of DPN than those on placebo, with an associated risk reduction in amputations of 37% (15). Fenofibrate may also be effective against DCN. PPAR-α knockout mice phenotypically have decreased corneal nerve density, impaired corneal sensitivity, and increased incidence of corneal lesions (16). The same study found that treatment with systemic fenofibrate significantly ameliorated the loss of corneal nerve fibers and restored glial cell–derived neurotrophic factor levels in the corneal epithelial and subbasal nerve plexus (16). These results suggest that PPAR-α agonists may have therapeutic potential for DCN. However, to our knowledge, the therapeutic effects of PPAR-α agonists against DCN have not been investigated and confirmed in a clinical trial. In the current study, we evaluated the potential effects of oral fenofibrate on the prevention of corneal nerve degeneration and the stimulation of corneal nerve regeneration in patients with type 2 diabetes. We also investigated the underlying mechanisms of the therapeutic effects with comprehensive tear neuromediator and proteomic analysis.

RESEARCH DESIGN AND METHODS

Study Design and Population

This was a single-arm, open-label, interventional study conducted at the Singapore National Eye Centre and Singapore General Hospital. Approval for the study was granted by the institutional review board of SingHealth, Singapore (ref. no. 2020/2050 and R1678/1/2020), and the study was conducted in accordance with the Declaration of Helsinki.

A total of 30 individuals with type 2 diabetes and 20 age-matched healthy control subjects were recruited from October 2020 to October 2021. Patients with diabetic nephropathy were recruited from the Singapore General Hospital's Diabetes and Metabolism Centre. Adults (≥21 years) with type 2 diabetes of at least 3 months duration and mild to moderate diabetic nephropathy, defined as a diminished creatinine clearance time (CCT) between 30 and 60 mL/min and/or albuminuria, were invited to participate. Patients had to have an HbA_{1c} of <9% (<75 mmol/mol) with no significant changes in the dosages of their lipid- and glucose-lowering agents in the past 3 months. Patients were excluded if they had severe renal impairment (CCT <30 mL/min) or received renal replacement therapy. They were also excluded if they had any non–diabetes-related renal glomerular disease, chronic liver disease, or significant alcohol intake. Patients with concurrent use of substances that would interfere with the intervention drug (e.g., tacrolimus, bile acid sequestrants, systemic steroids) were excluded as well. The full list of the inclusion and exclusion criteria for the diabetes cohort is detailed in Table 1. Control subjects comprised volunteers who were free of any health problems, were not on any long-term medications, and had no corneal pathology and history of ocular or corneal surgery.

Fenofibrate Treatment

Eligible subjects were treated with oral fenofibrate for 30 days. Fenofibrate is contraindicated in individuals with severe renal impairment (CCT <30 mL/min), and dose adjustment is required in the presence of renal impairment. The dosages of fenofibrate in this trial were based on the local drug regulatory authority's renal dosing recommendation. Subjects with a CCT >60 mL/min were treated with fenofibrate at 300 mg/day, and subjects with a CCT of 30–59 mL/min were treated with fenofibrate at 100 mg/day.

Patient age, diabetes duration, HbA_{1c}, and BMI were recorded. Additionally, blood tests were done to assess their pre- and postlevels of HDL, TGs, LDL, cholesterol, and fasting glucose. Neuropathic ocular surface assessment, in vivo confocal microscopy (IVCM) scans for corneal nerve plexuses and epithelial cells, tear neuromediator, and proteomic analysis were performed before and after treatment.

Table 1—Inclusion and exclusion criteria for the patients with diabetes

Inclusion criteria	≥21 years of age
	Type 2 diabetes defined by
	Fasting plasma glucose >7.0 mmol/L, or
	Symptoms of hyperglycemia with plasma glucose >11.1 mmol/L, or
	2-h plasma glucose >11.1 mmol/L after a 75-g oral glucose load
	Known type 2 diabetes duration >3 months
	HbA_{1c} <9% (<75 mmol/mol) within 3 months prior to enrollment
	Mild to moderate renal impairment, defined as more than one measurement in the past year with
	Urine microalbumin-to-creatinine ratio >3.3 mg/mmol creatinine, or
	Urine total protein-to-creatinine ratio (PCR) >0.2 g/urine creatinine, or
	creatinine clearance time 30–60 mL/min
	No change in dose of diabetes medication by more than twofold or new agents added within the previous 3 months
	No change in dose of lipid-lowering medications by more than twofold or new agents added within the previous 3 months
	Capable of providing informed consent
Exclusion criteria	Type 1 diabetes
	Known intolerance or allergic to statins, fenofibrate, peanut, arachis oil, soybean lecithin, or related products
	Concurrent use of medications that would interfere with the intervention drug: fibrates, colchicine, nicotinic acid, cyclosporine, tacrolimus, amodiaquine, bile acid sequestrants, chenodiol, ciprofibrate, oral anticoagulants (vitamin K antagonist, factor Xa inhibitors), antiobesity medications (phentermine, orlistat), systemic steroids (prednisolone, hydrocortisone, dexamethasone)
	Any ongoing acute medical illness
	Severe renal impairment defined as CCT <30 mL/min or renal replacement therapy
	Presence of any non-diabetes renal glomerular disease
	Serum ALT or AST greater than two times the upper limit of normal
	Chronic liver disease (e.g., hepatitis B, hepatitis C, autoimmune hepatitis, hemochromatosis)
	Previous pancreatitis
	Failure to obtain informed consent from patient

IVCM Scans for Corneal Nerves and Corneal Epithelium

Laser scanning IVCM (HRT3 with Rostock Corneal Module; Heidelberg Engineering, Heidelberg, Germany) was performed by an experienced technician masked to the study group assignment as previously described (17). Briefly, scans were obtained at the center of the patient's cornea first. The patient was then instructed to fixate on a light source in various directions with the contralateral eye to stabilize the scanning view, and the superior, inferior, nasal, and temporal region (each ∼3 mm away from the corneal apex) were also scanned. The scanned depth was from the superficial corneal epithelium to midstroma, at ∼350 μm. The time of image acquisition was 10 frames/s, and the field of view was 400 × 400 μm.

IVCM Image Analysis

To avoid observer bias, the images were deidentified prior to image analysis. For the corneal nerve analysis, five best-focused and most representative images of the subbasal nerves were selected for each scanned area. Each main nerve trunk and nerve branch was selected only once. These 25 micrographs selected for each eye were analyzed by an automated software program (ACCMetrics; University of Manchester, Manchester, U.K.) (18) for the following seven nerve parameters: *1*) corneal nerve fiber density (CNFD) (the number of fibers/mm^2, each frame area = 0.16033 mm^2), *2*) corneal nerve branch density (CNBD) (the number of branch points on the main fibers/mm^2), *3*) corneal nerve fiber length (CNFL) (total length of fiber mm/mm^2), *4*) corneal nerve fiber total branch density (CTBD) (total number of branch points/mm^2), *5*) corneal nerve fiber area (CNFA) (total nerve fiber area mm^2/mm^2), *6*) corneal nerve fiber width (CNFW) (average nerve fiber width mm/mm^2), and *7*) nerve fiber fractal dimension (CFracDim) (metric of corneal nerve morphology to measure the spatial loss of nerves) (19).

For the corneal epithelial cells analysis, the five best-focused micrographs selected for each eye were analyzed using AIConfocal Rapid Image Evaluation System software (ARIES; ADCIS, Saint-Contest, Basse-Normandie, France), which automatically calculates the cell density (μm^{-2}), average cell size (μm^2), and cell circularity (20).

Clinical Neuropathic Ocular Surface Assessments

A handheld Cochet-Bonnet esthesiometer (Luneau Ophthalmologie, Paris, France) containing a thin retractor nylon monofilament was used to assess the patients' corneal sensitivity. The 6.0-cm adjustable nylon filament was applied perpendicularly to the central and peripheral four quadrants of the subject's cornea, starting from 6.0 cm and progressively reducing in 5-mm steps until the first

response occurred (total scales 0–30 cm for five areas). Schirmer I test was performed by placing the Schirmer strips (Clement Clarke, Essex, U.K.) over the inferior temporal one-half of the lower lid margin in both eyes, without prior anesthesia, and the wet length (mm) after 5 min was recorded (21). Tear breakup time (TBUT) was evaluated by placing a single sterile fluorescein strip over the inferior fornix. The time interval between eye opening and the appearance of the first dry spot in the tear film was subsequently recorded (22). Ocular surface integrity was evaluated with fluorescence dye under the slit lamp using the cobalt blue illumination. Ocular surface staining was graded with the Oxford grading scale, ranging from 0 (absence of staining) to 5 (severe staining) (23). Corneal punctate staining was examined using the National Eye Institute (NEI) scale by dividing the cornea into five sections and assigning a value from 0 (absent) to 3 (severe) to each section, based on the amount, size, and confluence of the punctate lesions, for a maximum of 15 points.

Tear and Plasma Neuromediator Analysis

The strips collected from the Schirmer I test were stored at −80°C until the day for analysis. For tear neuromediator analysis, ELISA was performed. The wetted part of each Schirmer strip was first cut into small pieces and submerged in 200 μL of ice-cold tear elution buffer containing 0.55 mol/L NaCl, 0.33% Tween 20, 0.55% BSA, and 1× protease inhibitor. Tear samples were then homogenized by sonication for 20 s, followed by overnight incubation at 4°C with gentle shaking at 450 rpm. The homogenization step was repeated once before centrifugation at 11,000 rpm at 4°C for 20 min (24). The tear proteins containing clear supernatants were collected and stored at −80°C until ELISA analysis.

For plasma neuromediator analysis, blood from each patient at each visit was collected in EDTA-anticoagulated tubes, followed by centrifugation at 3,000 rpm at 4°C for 10 min. The plasma was collected and stored at −80°C until ELISA analysis.

The level of tear and plasma neuromediators, including substance P (SP), calcitonin gene-related peptide (CGRP), neuropeptide Y (NPY), and NGF, was analyzed separately using ELISA kits according to the manufacturer's instructions. The details of the dilution factors and kit information are provided in Supplementary Table 1. The optical density measurement was read at 450 nm using an Infinite M200 plate reader (Tecan, Männedorf, Switzerland), and optical density reading at 540 nm was set as the reference. The final concentrations of each analyte were interpolated from the standard curve using GraphPad Prism 8 software (GraphPad Software, San Diego, CA).

Tear Proteomic Analysis

Quantitative tear proteomic analysis was performed as previously described (25). The Schirmer strips were cut into small pieces, and 100 μL of lysis buffer was added and mixed in a ThermoMixer for 1.5 h at 20°C. The total protein concentration was measured using Bio-Rad DC Protein assay. One hundred micrograms of eluted tear proteins were reduced, alkylated, tryptic digested, and desalted using the reagents from EasyPep Mini Sample Prep Kits (Thermo Fisher Scientific, San Jose, CA). The total peptide amount was quantified with a fluorometric peptide quantification kit. The peptide sample was dried with SpeedVac and resuspended in 2% acetonitrile with 0.1% formic acid containing iRT (1:10 ratio; Biognosys). All peptide samples (1 μg of total peptides per sample) were analyzed using an EASY-nLC 1200 system coupled to an Orbitrap Exploris 480 mass spectrometer via an EASY-Spray source. For liquid chromatography separation, an Acclaim PepMap 100 C18 was used as the precolumn and a PepMap RSLC C18 as the analytical column. Peptides were separated by a 60-min gradient using 0.1% formic acid as buffer A and 80% acetonitrile in 0.1% formic acid as buffer B. The reagent, kits, and columns were purchased from Thermo Fisher Scientific. Quantitative proteomic analysis was performed using data independent acquisition (DIA) experiments. In total, 19 windows of 45.7 Da were used with an overlap of 3 Da. The normalized automatic gain control target value for fragment spectra was set at 1,000%, and maximum injection time mode was set to auto. DIA data were processed using library-free directDIA workflow in Spectronaut 15 (Biognosys).

Raw protein abundance values were derived after fragment ions were selected for quantification based on default quality control criteria as implemented in mapDIA (26). The downstream data analysis, data visualization, and Gene Ontology term enrichment were performed using custom scripts in R (64-bit, version 4.1.1). The raw abundance data were median normalized and log transformed for all statistical analyses. Based on the proteomics data set, pathway enrichment analysis was performed with gene set enrichment analysis (GSEA) (27) using the Kyoto Encyclopedia of Genes and Genomes database. The enrichment score (ES) corresponds to the (weighted) Kolmogorov-Smirnov statistic and reflects the degree to which the gene (protein) in a gene (protein) set is upregulated (positive ES) or downregulated (negative ES).

Statistical Analysis

The required sample size was calculated based on the pilot data of the primary outcome, which was CNFD, from five patients. The mean CNFD was 9.5 ± 5.1 fibers/mm^2 and 12.3 ± 5.3 fibers/mm^2 before and after treatment, respectively. Hence, a sample size of 22 patients, with a power of ≥80% and at a 5% level of significance, was sufficient to detect the difference before and after treatment. Considering a 15% rate of loss to follow-up, we recruited 30 patients with diabetes. Linear mixed models were used to analyze the data before and after treatment from both eyes, as well as the data of control subjects and patients before treatment, to take into account the correlation of the paired time points and both eyes. Linear mixed models were also

used to evaluate the association between the neuromediator and nerve profiles. All data are expressed as mean ± SD. The statistical analysis was performed using Stata 17 (StataCorp, College Station, TX), and $P < 0.05$ was considered significant.

Data and Resource Availability

All data generated or analyzed during this study are included in the published article and its online supplementary files. Resources will be made available upon request.

RESULTS

Demographic and Clinical Characteristics of the Study Populations

Of the 30 patients with diabetes, 21 (70%) and 9 (30%) were prescribed oral fenofibrate 100 mg/day and 300 mg/day, respectively. The mean age was 60.8 ± 9.3 years, and the majority (80.8%) were men and Chinese. Table 2 shows the clinical and demographic characteristics of the patients with diabetes and control subjects. Patients with diabetes had significantly higher HbA_{1c} and LDL levels (both $P < 0.001$) compared with the control subjects. The serum TGs decreased from 1.8 ± 1.1 to 1.4 ± 0.8 mmol/L ($P = 0.002$) after fenofibrate treatment, suggesting good adherence to the intervention drug. The other baseline characteristics were comparable to the control group (all $P > 0.05$).

Oral Fenofibrate Significantly Improved Corneal Nerve Metrics in Diabetes

Compared with the control subjects, patients with diabetes had significantly lower CNFD ($P = 0.04$) and CNFL ($P = 0.03$) and higher CNFW ($P = 0.03$). Their corneal nerves were more tortuous and had a greater number of nerve beadings (Fig. 1*A*). After fenofibrate treatment, CNFD significantly increased from 9.5 ± 6.2 to 12.6 ± 4.4 fibers/mm^2 ($P = 0.01$) and was restored to the level comparable to the control group (12.3 ± 6.0 fibers/mm^2). Following treatment, CNFW significantly decreased from 0.024 ± 0.001 to 0.022 ± 0.001 mm/mm^2 ($P = 0.01$), suggesting less swelling of the nerve fibers. There was also a trend of improvement in CNBD, CTBD, CNFA, and CFracDim, though it did not reach statistical significance (Table 3 and Fig. 2).

Oral Fenofibrate Effectively Improved Corneal Epithelial Morphology in Diabetes

Morphological improvement with a more regular cell border was observed in the corneal epithelial layers after treatment, as evidenced by a significant decrease in the circularity of the cells from 0.73 ± 0.02 to 0.72 ± 0.02 ($P = 0.04$) (Table 3). We also observed that the epithelial cell density became more compact along with a reduction in cell size (Fig. 1*B*) from 131.0 ± 22.1 to 127.1 ± 9.50 μm^2 (Table 3). After treatment, the epithelial cell parameters improved to a level close to those of control subjects (Table 3 and Fig. 2*H–J*).

Clinical Ocular Surface Function Was Significantly Restored After Oral Fenofibrate Treatment

Corneal sensitivity (24.6 ± 1.8 vs. 27.5 ± 1.4 mm; $P < 0.001$), TBUT (5.7 ± 1.5 vs. 8.1 ± 1.7 s; $P < 0.001$), ocular surface Oxford score (0.8 ± 0.8 vs. 0.3 ± 0.6; $P = 0.004$), and corneal staining NEI score (1.2 ± 1.1 vs. 0.2 ± 0.5; $P = 0.001$) were significantly worse in the patients with diabetes than control subjects (Table 4). After fenofibrate treatment, ocular surface superficial punctate keratopathy, which stained green with

Table 2—Demographic characteristics and clinical parameters of patients with diabetes and control subjects

Demographic characteristic and clinical parameter	Patients with diabetes: Before fenofibrate treatment	Patients with diabetes: After fenofibrate treatment	P*	Control subjects	P†
Age (years)	60.8 ± 9.3			63.7 ± 7.0	0.26
Sex, *n* (%)					
Male	21 (80.8)			11 (55)	
Female	5 (19.2)			9 (45)	
Body weight (kg)	76.9 ± 18.3			75.7 ± 16.8	0.55
Body height (m)	1.6 ± 0.1			1.7 ± 0.1	0.28
BMI (kg/m^2)	28.2 ± 4.7			27.8 ± 4.6	0.93
Fasting blood glucose (mmol/L)	7.4 ± 1.6	7.0 ± 2.0	0.165	6.2 ± 0.4	0.18
HbA_{1c} (%)	7.6 (60 mmol/mol) ± 1.0			6.2 (44 mmol/mol) ± 1.1	**<0.0001**
Total cholesterol (mmol/L)	3.9 ± 0.7	3.9 ± 0.6	0.47		
HDL (mmol/L)	1.2 ± 0.3	1.2 ± 0.3	0.52	1.5 ± 0.4	**0.05**
LDL (mmol/L)	1.9 ± 0.7	2.0 ± 0.7	0.24	1.3 ± 1.3	**<0.0001**
TGs (mmol/L)	1.8 ± 1.1	1.4 ± 0.8	**0.002**	1.7 ± 0.8	0.80

Data are mean ± SD unless otherwise indicated. Boldface indicates significance at $P < 0.05$. *Comparisons are between the data before and after fenofibrate treatment. †Comparisons are between the data of the control subjects and patients with diabetes before fenofibrate treatment.

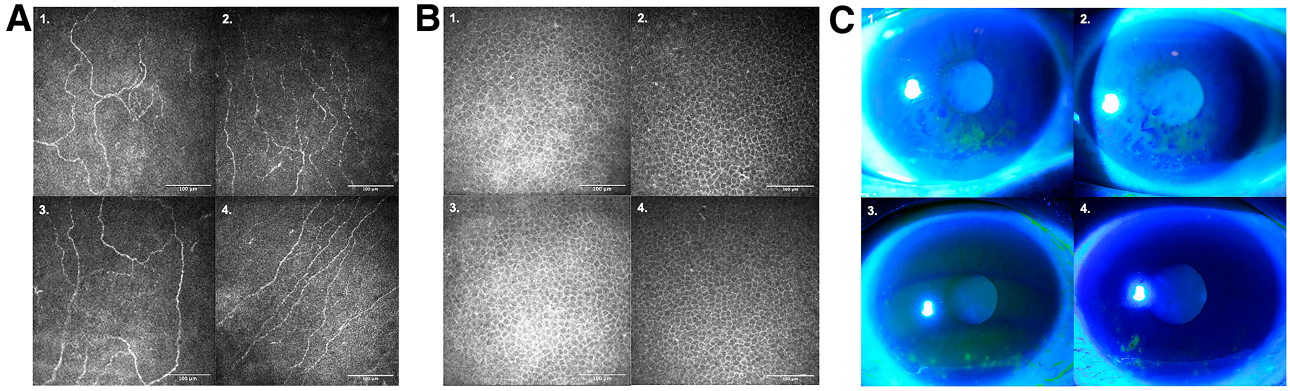

Figure 1—Representative IVCM and slit-lamp images of the study patients before and after treatment. *A*: Images of corneal subbasal nerve plexus before (1 and 2) and after (3 and 4) fenofibrate treatment, demonstrating an increase in CNFD. IVCM images show beadings (2) with abrupt ending of nerve fibers before treatment and continuous nerve fibers (4) after treatment. *B*: IVCM images of corneal epithelial cells before (1 and 2) and after (3 and 4) fenofibrate treatment, demonstrating a morphological improvement and restoration of regular polygonal shape along with a reduction in cell size. *C*: Slit-lamp images of the ocular surface superficial punctate keratopathy, which was stained green with fluorescein dye under cobalt blue light before (1 and 2) and after (3 and 4) fenofibrate treatment, demonstrating a significant reduction in punctate keratopathy and a more stable tear film.

fluorescein dye under cobalt blue light (Fig. 1*C*), was significantly reduced, as also evidenced by the significant reduction in Oxford and NEI scores. The mean Oxford score significantly decreased from 0.8 ± 0.8 to 0.6 ± 0.6 (P = 0.01). The mean NEI scores also significantly improved from 1.2 ± 1.1 to 0.7 ± 0.6 (P = 0.008). The tear film became significantly more stable (Fig. 1*C*), as demonstrated by the significant improvement in TBUT from 5.7 ± 1.5 to 6.2 ± 1.8 s (P = 0.006) (Fig. 2).

Oral Fenofibrate Suppressed Ocular Surface Neuroinflammation in Diabetes

The patients with diabetes had a significantly lower tear SP (P = 0.05) and a significantly higher NGF level (P = 0.04) than the control subjects. After treatment, the tear SP levels significantly increased from 1,239.4 ± 719.2 to 1,669.0 ± 948.4 pg/mL (P = 0.03) (Table 4). Of note, the changes in tear SP level were significantly associated with an increase in CNFD (β = 0.003; P = 0.013). There was no significant alteration in the CGRP, NPY, and NGF levels in tears after treatment (Table 4).

The SP level in plasma was 228.3 ± 87.8 and 203.9 ± 76.6 pg/mL before and after treatment, respectively (P = 0.08). The CGRP levels in plasma were 77.0 ± 15.4 and 77.8 ± 12.0 pg/mL before and after treatment (P = 0.86). Fenofibrate did not alter blood neuromediator profiles.

Tear Proteomic Profiles and Pathway Enrichment Analysis

In the diabetes group, apolipoprotein A-IV (APOA4) ($\log_2$ fold change [$\log_2$FC] = 2.28), and serum amyloid A-1 protein (SAA1) ($\log_2$FC = −3.82), both related to inflammation, were significantly increased (Fig. 3*A*). Elevated APOC1 ($\log_2$FC = 2.68) and complement C1q subcomponent subunit A (C1QA) proteins, which are essential for several complement-mediated activities, were also observed

Table 3—In vivo confocal microscopy imaging analysis of patients with diabetes and control subjects

	Patients with diabetes				
IVCM parameter	Before fenofibrate treatment	After fenofibrate treatment	P*	Control subjects	P†
Corneal subbasal nerves					
CNFD	9.5 ± 6.2	12.6 ± 4.4	**0.01**	12.3 ± 6.0	**0.04**
CNBD	9.6 ± 10.3	11.2 ± 7.4	0.45	10.4 ± 8.0	0.80
CNFL	7.7 ± 3.2	8.7 ± 2.4	0.11	9.7 ± 3.4	**0.03**
CTBD	20.0 ± 14.6	20.8 ± 9.1	0.77	20.9 ± 13.1	0.74
CNFA	0.004 ± 0.001	0.004 ± 0.001	0.97	0.004 ± 0.001	0.93
CNFW	0.024 ± 0.001	0.022 ± 0.001	**0.01**	0.022 ± 0.001	**0.03**
CFracDim	1.39 ± 0.06	1.40 ± 0.04	0.11	1.40 ± 0.04	0.12
Corneal epithelial cells					
Density (cells/μm^2)	0.0078 ± 0.0005	0.0100 ± 0.0003	0.22	0.0079 ± 0.0006	0.54
Average size (μm^2)	131.0 ± 22.1	127.1 ± 9.50	0.31	128.4 ± 10.1	0.71
Circularity	0.73 ± 0.016	0.72 ± 0.021	**0.04**	0.72 ± 0.097	0.11

Data are mean ± SD. Boldface indicates significance at $P < 0.05$. *Comparisons are between the data before and after fenofibrate treatment. †Comparisons are between the data of the control subjects and the patients with diabetes before fenofibrate treatment.

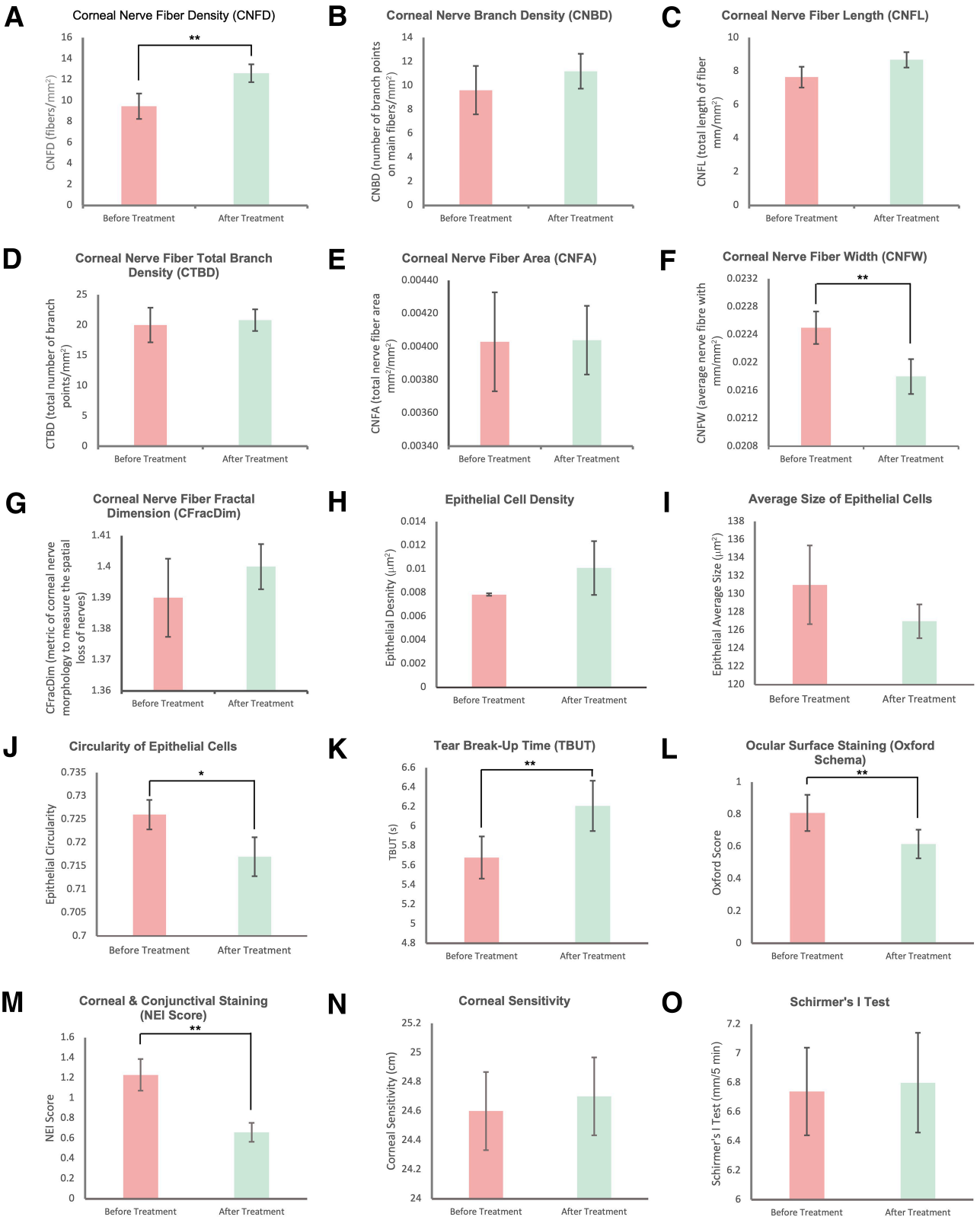

Figure 2—Bar charts showing the corneal nerve, epithelial cells, and ocular surface clinical parameters of patients with diabetes before and after treatment. CNFD (*A*), CNBD (*B*), CNFL (*C*), CTBD (*D*), CNFA (*E*), CNFW (*F*), CFracDim (*G*), epithelial cell density (*H*), average size of epithelial cells (*I*), circularity of epithelial cells (*J*), TBUT (*K*), ocular surface staining (Oxford score) (*L*), corneal staining (NEI score) (*M*), corneal sensitivity (*N*), and Schirmer I test (*O*). *$P < 0.05$, **$P \leq 0.01$.

Table 4—Clinical ocular surface parameter and tear neuromediator analysis of patients with diabetes and control subjects

Parameter	Patients with diabetes				
	Before fenofibrate treatment	After fenofibrate treatment	*P**	Control subjects	*P*†
Ocular surface parameters					
Corneal sensitivity	24.6 ± 1.8	24.7 ± 1.8	0.16	27.5 ± 1.4	**<0.001**
TBUT	5.7 ± 1.5	6.2 ± 1.8	**0.006**	8.1 ± 1.7	**<0.001**
Schirmer I test	6.7 ± 2.1	6.8 ± 2.3	0.84	6.7 ± 2.2	0.88
Ocular surface staining (Oxford score)	0.8 ± 0.8	0.6 ± 0.6	**0.01**	0.3 ± 0.6	**0.004**
Cornea staining (NEI score)	1.2 ± 1.1	0.7 ± 0.6	**0.008**	0.2 ± 0.5	**0.001**
Tear neuromediator					
SP (pg/mL)	1,239.4 ± 719.2	1,669.0 ± 948.4	**0.03**	2,672.0 ± 467.3	**0.05**
CGRP (ng/mL)	1.3 ± 0.6	1.4 ± 0.6	0.49	2.6 ± 1.1	0.08
NPY (ng/mL)	1.0 ± 0.4	1.1 ± 0.5	0.10	1.3 ± 0.5	0.37
NGF (pg/mL)	10.2 ± 11.0	10.0 ± 11.3	0.91	5.4 ± 3.8	**0.04**

Data are mean ± SD. Boldface indicates significance at $P < 0.05$. *Comparisons between the data before and after fenofibrate treatment. †Comparisons between the data of the control subjects and patients with diabetes before fenofibrate treatment.

($log_2FC = 3.08$) (Fig. 3*A*). The top 25 tear proteins that were significantly up- and downregulated in the eyes of patients with diabetes versus control subjects are listed in Table 5 and Supplementary Fig. 1*A*. These significant dysregulated protein expressions were linked to significantly downregulated cholesterol (ES −0.75; $P = 0.001$), carbohydrate (ES −0.93; $P = 0.002$), fat (ES −0.80; $P = 0.008$), and protein (ES −0.94; $P = 0.01$) metabolism. In particular, neuroactive ligand-receptor interaction (ES −0.89; $P = 0.04$) and PPAR signaling pathway (ES −0.67; $P = 0.01$) were significantly downregulated in the patients with diabetes (Fig. 3*A* and Table 6).

When comparing tear proteomic profiles before and after fenofibrate treatment, β-galactoside α-2,6-sialytransferase 1 (ST6GAL1) ($log_2FC = 1.42$), human tetratricopeptide repeat protein 9A (TCC9A) ($log_2FC = 0.75$), and ras-related protein (RAB5A) ($log_2FC = 0.63$), all involved in the regulation of nervous system function, were significantly increased after treatment (Fig. 3*B*). Significant upregulation of suppressor of mothers against decapentaplegic homolog 1 (SMAD1) ($log_2FC = 1.72$), which is important for the maintenance of neural cells (28), was also observed after treatment. On the other hand, cytochrome c oxidase assembly factor 6 homolog (COA6) ($log_2FC = -2.66$), which is involved in the transcriptional network in neurons (29), was significantly downregulated. Lamin-B1 (LMNB1) ($log_2FC = -1.44$), a scaffolding component of nuclear envelope, was also significantly downregulated (Fig. 3*B*). Table 5 and Supplementary Fig. 1*B* list the top 25 tear proteins that are significantly up- and downregulated after treatment. Upon GSEA analysis, we found that three neuronal regulation–related pathways were significantly upregulated after treatment: *1*) MAPK signaling pathway (ES 0.53; $P = 0.009$), *2*) neurotrophin signaling pathway (ES 0.59; $P = 0.01$), and *3*) linoleic acid (LA) metabolism (ES 1.00; $P = 0.01$) (Table 6). Ribosome family was significantly downregulated (ES −0.67; $P = 0.002$). Fenofibrate treatment also significantly modulated cholesterol and fat metabolism (ES 0.77 [$P = 0.004$] and 0.90 [$P = 0.006$], respectively). Ocular surface complement and coagulation cascades (ES −0.78; $P = 0.001$), neutrophil extracellular trap formation (ES −0.69; $P = 0.001$), and platelet activation (ES −0.66; $P = 0.01$) were significantly downregulated after treatment (Fig. 3*B* and Table 6).

DISCUSSION

In this clinical trial, we demonstrated for the first time the neurotrophic effect of oral fenofibrate on diabetic corneas. The beneficial effects on neuropathic ocular surface are evidenced by the significant improvement in CNFD, CNFW, epithelial cell morphology, and tear SP level. These further contributed to an objective improvement in the clinical ocular surface function through an improvement in tear stability and the reduction of corneal and conjunctival punctate keratopathy. We also found that treatment with fenofibrate was associated with alterations in three pathways: *1*) neuronal pathway, *2*), lipid modulation, and *3*) anti-inflammation and anticoagulation.

Treatment with oral fenofibrate improves corneal nerve metrics in diabetic corneas. At baseline, we observed a significantly lower CNFD and CNFL, as well as significantly higher CNFW, in the diabetes cohort compared with the age-matched control cohort. This finding is supported by previous literature showing that CNFD and CNFL were significantly reduced in patients with diabetes (30,31). Thickening of subbasal nerves found in diabetic corneas (32) may be indicative of the progressive deposition of advanced glycation end products and an increase in DPN severity (6,33). After fenofibrate treatment, CNFD and CNFW improved significantly, with CNFD restored toward the level of control subjects. These findings indicate that fenofibrate leads to the regeneration of nerve fiber and a reduction in nerve edema. Moreover, we observed a trend of improvement in CFracDim posttreatment, indicating a decrease in the spatial loss of nerve fibers. Fenofibrate treatment also improved the morphology of the epithelial cells in terms of cell circularity. The corneal subbasal plexus is thought to contribute to a healthy

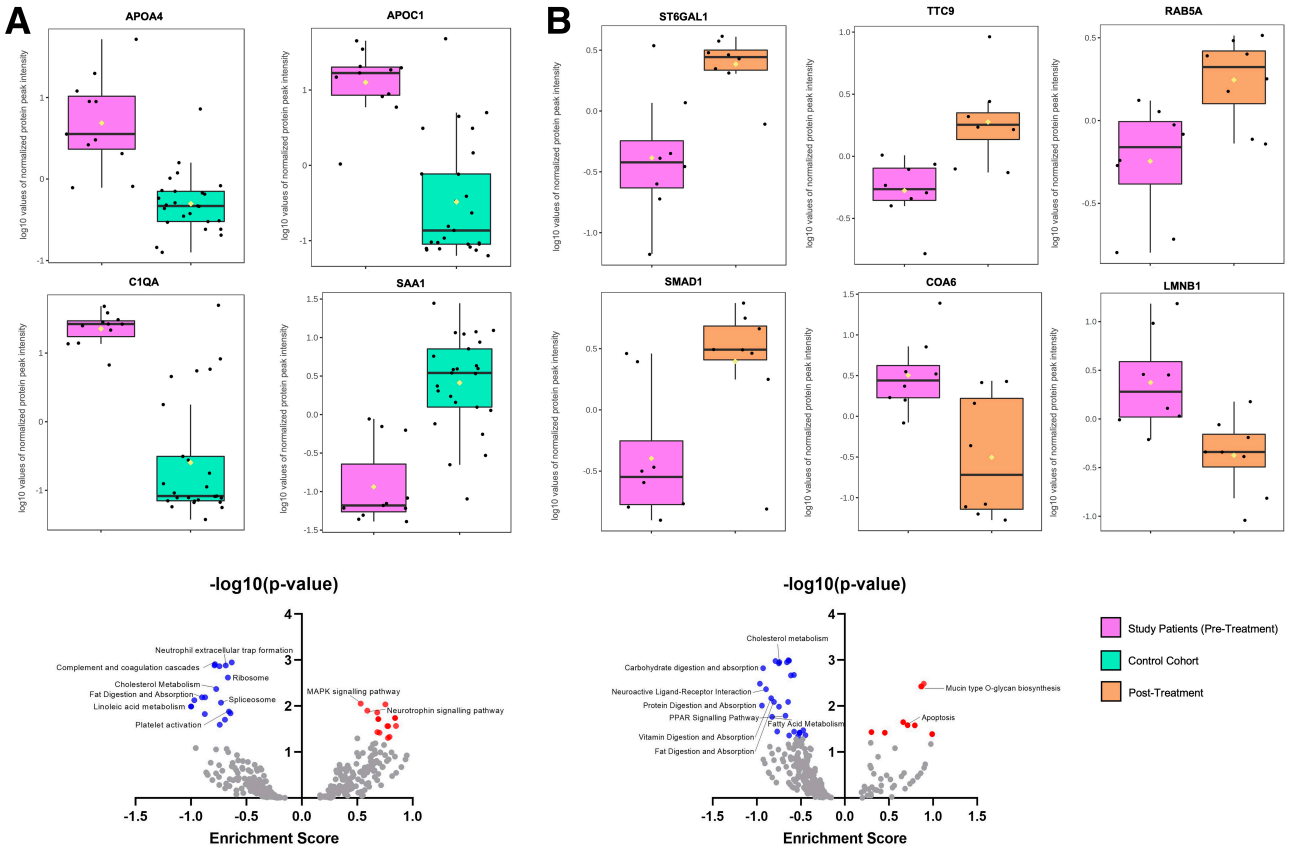

Figure 3—Box-and-whisker plots showing the representative tear proteins of the patients with diabetes and scatter plots showing the GSEA. *A*: Plots demonstrate a significantly upregulated APOA4, APOC1, and C1QA and a significantly downregulated SAA1 in patients with diabetes (before treatment) compared with control subjects. *B*: After fenofibrate treatment, there was a significantly upregulated ST6GAL1, TCC9A, RAB5A, and SMAD1 and a significantly downregulated COA6, and LMNB1. The *y*-axis represents the $\log_{10}$ values of normalized protein peak intensity. The box ranges from the first quartile to the third quartile of the distribution of proteins, and the range represents the interquartile range. The median of the data set is indicated by a line across the box. Top whiskers represent values higher than the median, and bottom whiskers represent values lower than the median. The vertical line on the box plot extends from the minimum to the maximum of the data set. Scatter plots for GSEA results (ES and $-\log_{10}$ [*P* value]) showing the enrichment pathways ($P < 0.05$) in patients with diabetes vs. control subjects (*A*) and patients with diabetes before and after treatment (*B*). Red dots represent the significantly upregulated pathways, and blue dots represent the significantly downregulated pathway.

epithelial surface by providing trophic influences and maintaining epithelial metabolism (34). Several studies have shown that hyperglycemia compromises epithelial barrier function, resulting in morphological changes to the corneal epithelial cells (35). Neurotrophic factors, such as epithelial growth factor and ciliary neurotrophic factor, have been shown to promote corneal epithelial wound healing (36). In line with these observations, the upregulation of neurotrophin signaling and neurotrophic factors could explain the posttreatment improvement in corneal epithelial morphology.

Clinically, the diabetes cohort had significantly worse corneal sensitivity, TBUT, and corneal and ocular surface punctate keratopathy compared with the control cohort. Diabetes-induced denervation reduces blink reflex, trophic support, and the viability of the corneal epithelial cells, putting patients at an increased risk of ocular surface damage (36). Studies have also suggested that ocular surface dysfunction is correlated with the duration and severity of diabetes (37,38). We found that fenofibrate promoted ocular surface homeostasis, as evidenced by the significant improvement in TBUT and Oxford and NEI scores. The stimulation of corneal nerves also promotes lacrimal gland secretions and maintains tear volume and composition (39). Hence, the improvement in corneal nerve metrics would also provide favorable effects on patients' TBUT and ocular surface integrity. We did not observe significant changes in Schirmer values after treatment, and this may be due to the high variability and low repeatability of Schirmer I tests (40). While fenofibrate improved several nerve parameters, corneal sensitivity remained unchanged, highlighting the issue that the current clinical evaluation tool (i.e., corneal esthesiometer) is too crude to detect subtle nerve changes. A greater degree of neuronal restoration may also be needed before any clinically appreciable improvement in corneal sensitivity could be observed.

Neuromediators, which are released in response to nerve damage or stimulation, are crucial in maintaining ocular surface homeostasis. SP stimulates the proliferation of

Table 5—Top 25 significantly upregulated or downregulated tear proteins

	Protein name	FC	Log_2FC	*P*
Patients with diabetes* vs. control subjects				
1	Neuroplastin (NTPN)	8.7939	3.1365	0.0000
2	APOC1	6.4218	2.6830	0.0001
3	Aminoacyl tRNA synthase complex–interacting multifunctional protein 2 (AIMP2)	12.6270	3.6585	0.0001
4	C1QA	8.4485	3.0787	0.0000
5	APOA4	4.8479	2.2774	0.0001
6	Serine/threonine-protein phosphatase PP1-α catalytic subunit (PPP1CA)	0.4511	−1.1485	0.0002
7	AP-1 complex subunit β-1 (AP1B1)	0.5234	−0.9341	0.0001
8	Glycogen phosphorylase, brain form (PYGB)	0.2565	−1.9631	0.0001
9	Radixin (RDX)	0.2333	−2.1000	0.0001
10	Zinc finger protein 185 (ZNF185)	0.4224	−1.2435	0.0000
11	Twinfilin-1 (TWF1)	0.4425	−1.1762	0.0001
12	Zinc finger protein 185 isoform A (ZNF185.1)	0.3804	−1.3944	0.0001
13	Proteasome subunit β type-9 (PSMB9)	0.4084	−1.2920	0.0001
14	Epidermal growth factor receptor kinase substrate 8–like protein 2 (EPS8L2)	0.2899	−1.7865	0.0002
15	14-3-3 protein θ (YWHAQ)	0.3871	−1.3691	0.0002
16	Caspase-7 (CASP7)	0.2851	−1.8106	0.0002
17	Calpain-1 catalytic subunit (CAPN1)	0.3298	−1.6002	0.0002
18	StAR-related lipid transfer protein 5 (STARD5)	0.0783	−3.6748	0.0001
19	Proteasome subunit α type-1 (PSMA1)	0.4644	−1.1066	0.0001
20	Tropomyosin α-4 chain (TPM4)	0.5127	−0.9639	0.0001
21	Claudin-4 (CLD4)	0.3036	−1.7198	0.0001
22	Carcinoembryonic antigen–related cell adhesion molecule 6 (CEACAM6)	0.3218	−1.6356	0.0000
23	Eukaryotic translation initiation factor 3 subunit C (EIF3C)	0.6134	−0.7052	0.0001
24	SAA1	0.0710	−3.8159	0.0001
25	Transitional endoplasmic reticulum ATPase (VCP)	0.4953	−1.0137	0.0001
Patients with diabetes after fenofibrate treatment				
1	Cytochrome P450 2S1 (CYP2S1)	0.2775	−1.8495	0.0033
2	LMNB1	0.3680	−1.4421	0.0048
3	COA6	0.1584	−2.6580	0.0059
4	Malectin (MLEC)	0.5856	−0.7719	0.0109
5	Mannose-6-phosphate isomerase (MPI)	1.8316	0.8731	0.0112
6	γ-Soluble NSF attachment protein (NAPG)	1.5528	0.6349	0.0056
7	Vacuolar protein sorting–associated protein 37C (VPS37C)	15.0380	3.9105	0.0027
8	Fucose-1-phosphate guanylyltransferase (FPGT)	3.6539	1.8694	0.0027
9	TCC9A	1.6769	0.7458	0.0023
10	Ankyrin repeat domain-containing protein 13A (ANKRD13A)	4.4458	2.1525	0.0020
11	Queuosine salvage protein (C9orf64)	1.6086	0.6858	0.0009
12	ST6GAL1	2.6667	1.4151	0.0016
13	SMAD1	3.2938	1.7198	0.0094
14	Dual-specificity MAPK 6 (MAP2K6)	2.5110	1.3283	0.0103
15	Ethanolamine-phosphate cytidylyltransferase (PCYT2)	1.9035	0.9287	0.0101
16	Hydroxyacylglutathione hydrolase, mitochondrial (HAGH)	1.7263	0.7877	0.0099
17	Galectin-related protein (LGALSL)	1.7441	0.8025	0.0090
18	NSFL1 cofactor p47 (NSFL1C)	1.5332	0.6165	0.0086
19	Inosine triphosphate pyrophosphatase (ITPA)	1.8107	0.8566	0.0082
20	RAB5A	1.5487	0.6311	0.0059
21	Glucose 1,6-bisphosphate synthase (PGM2L1)	1.4341	0.5201	0.0059
22	Molybdopterin synthase sulfur carrier subunit (MOCS2)	5.6271	2.4924	0.0058
23	Exportin-7 (XPO7)	1.4661	0.5520	0.0057
24	eIF-2-α kinase activator (GCN1)	2.3882	1.2559	0.0026
25	Proteasome activator complex subunit 2 (PSME2)	1.5803	0.6602	0.0038

*Status before oral fenofibrate treatment.

epithelial cells and promotes diabetic corneal epithelial wound healing via neurokinin-1 receptors (41). The reduction in tear SP levels is associated with an increase in DPN severity (42) and predisposes peripheral nerves to early neuropathic changes (42). In our study, we found that tear SP concentrations were significantly lower in patients with diabetes, and its level significantly increased after fenofibrate treatment. Notably, this increment in tear SP was significantly associated with the increase in CNFD, demonstrating that tear SP may serve as a surrogate biomarker for corneal nerve regeneration in concordance with previous studies illustrating a significant correlation between

Table 6—Top 10 significantly expressed pathways involved by significantly upregulated and downregulated proteins

	Pathway name	ES	*P*
Patients with diabetes vs. control subjects			
1	Cholesterol metabolism	−0.7484	0.001
2	Carbohydrate digestion and absorption	−0.9271	0.002
3	Mucin type *O*-glycan biosynthesis	0.8703	0.004
4	Neuroactive ligand-receptor interaction	−0.8933	0.004
5	Vitamin digestion and absorption	−0.8362	0.007
6	Fat digestion and absorption	−0.8040	0.008
7	Protein digestion and absorption	−0.9414	0.010
8	PPAR signaling pathway	−0.6747	0.016
9	Fatty acid metabolism	−0.8265	0.017
10	Apoptosis	0.7108	0.026
Patients with diabetes after fenofibrate treatment			
1	Complement and coagulation cascades	−0.7841	0.001
2	Neutrophil extracellular trap formation	−0.6868	0.001
3	Ribosome	−0.6669	0.002
4	Cholesterol metabolism	−0.7735	0.004
5	MAPK signaling pathway	0.5317	0.009
6	Fat digestion and absorption	−0.9012	0.006
7	Spliceosome	−0.7304	0.008
8	LA metabolism	0.9992	0.010
9	Neurotrophin signaling pathway	0.5903	0.013
10	Platelet activation	−0.6576	0.013

tear SP and CNFD (42,43). Tear NGF concentrations were also found to be significantly higher in the patients with diabetes than in control subjects, which could be due to *1*) a consequence of neuroinflammation (44), *2*) a compensatory reaction to decreased corneal nerves (44), *3*) an impaired uptake and transportation system of NGF in patients with diabetes (45,46), or *4*) a protective response to degenerative nerves (47).

Neuroactive ligands are important for the maintenance of protective corneal reflexes, support for epithelial regeneration, and the recovery of nervous function (48). We found a significantly downregulated neuroactive ligand-receptor interaction and PPAR signaling pathway in the patients with diabetes cohort, which could explain their clinical manifestations, such as decreased corneal sensitivity and superficial punctate keratopathy. More recently, a study demonstrated that PPAR-α levels were reduced in the corneas of diabetic mice, and the knockout of PPAR-α alone was sufficient to induce corneal nerve degeneration, impaired corneal sensitivity, and increased corneal lesions (16). The downregulation of PPAR-α thus plays a pathogenic role in diabetic keratopathy, which may be amendable to treatment using PPAR-α agonists such as fenofibrate.

The neuroprotective effects of fenofibrate are not fully understood but can occur via several mechanisms (Table 7). Based on our GSEA, oral fenofibrate stimulated the neurotrophin and MAPK signaling pathways as well as LA metabolism. Neurotrophins are essential for the modulation of corneal nerve branching, maintenance of corneal nerve density, and the success of nerve regeneration (49). The activation of MAPK mediates neurite outgrowth-promoting effects in vitro (50). Moreover, overexpression of LA metabolism generates γ-LA, which serves as an important constituent of neuronal membrane phospholipids and helps to preserve nervous blood flow to facilitate nerve regeneration (51). We also found that fenofibrate suppressed the expression of ribosome. Axonal ribosomes serve as a marker for diseased axons and indicate involvement in neurodegenerative disorders (52). Taken together, these data suggest that fenofibrate potentially attenuates neurodegeneration and enhances neuroprotection.

Elevated triglycerides are associated with corneal nerve damage in patients with small fiber neuropathy (53). We found that the metabolism of cholesterol and fatty acid was significantly downregulated in the diabetes cohort. As fenofibrate acts by lowering triglycerides and increasing HDL levels, this could explain the posttreatment improvement in DCN. A recent review demonstrated the mechanistic link between altered lipid metabolism and peripheral nerve dysfunction (54), suggesting the importance of lipid modulation in DCN. From the angle of drug discovery, fenofibrate stands in a more favorable position compared with other investigational drugs, as it is a drug prescribed routinely for the management of dyslipidemia.

We also found that fenofibrate significantly suppressed neutrophil extracellular trap formation, complement and coagulation cascades, and platelet activation pathways. Similarly, it was reported that topical PPAR-α treatment inhibits proinflammatory markers, suppresses inflammatory cells, and promotes corneal wound healing in the cornea of a rat alkali-burned model (55). The same study found that topical PPAR-α suppresses nuclear factor κB expression (55). The inhibition of nuclear factor κB has been reported to reduce neuroinflammation as well as stimulate neurogenesis (56), neuritogenesis (57), and axoneogenesis (58). In our study, we found that ST6GAL1, which regulates neutrophilic inflammatory response (59), increased following treatment. Furthermore, low platelet time and plateletcrit levels were found to have a significant association with poorer nerve conduction function and the presence of neuropathy in patients with type 2 diabetes (60). Collectively, these suggest that the suppression of inflammation and platelet activation are possible mechanisms of fenofibrate.

On the protein level, APOA4 was significantly upregulated in the diabetes cohort. Increased APOA4 was found in the early stages of nerve degeneration (61). This increase was postulated to be in response to denervation and chronic neuroinflammation due to hyperglycemia (62). SAA1, on the other hand, was significantly decreased in patients with diabetes, which is in agreement with a previous study (63). APOC1 and C1QA, which are both associated with inflammation and diabetic nephropathy (64,65), were significantly upregulated in the tears of the patients with diabetes. After treatment, there was an increase in the expression of neurotrophic receptors by the upregulation of TCC9A and RAB5A. TCC9A and RAB5A regulate neuronal plasticity

Table 7—Literature review of the effects of fenofibrate on neuropathy and neurodegeneration

Source	Study aims	Treatment	Proposed mechanisms and conclusion
Corneal neuropathy			
Matlock et al., 2020 (16)	To investigate the protective role of PPAR-α against diabetic keratopathy and corneal neuropathy.	Oral fenofibrate (0.014%) was given for 2–4 months to diabetic and nondiabetic rats, and 6 months to PPAR-α knockout mice.	To upregulate the expression BDNF and GDNF, thus regulating neuronal and glial cell development and differentiation, functions, remodeling, and regeneration. Conclusion: Fenofibrate prevented the incidence of spontaneous corneal epithelial lesions, restored neurotrophic factor levels in diabetic corneas, and protected against the degeneration of corneal nerve induced by diabetes.
Peripheral neuropathy			
Caillaud et al., 2021 (12)	To test the efficacy of fenofibrate in preventing the development of PIPN.	Oral fenofibrate (0.2% and 0.4%) was given to PIPN-induced mice for 2 weeks.	To reduce neuroinflammation via the induction of PPAR-α mRNA expression in the dorsal root ganglia and the reduction in inflammatory markers mediated by the PPAR-α–dependent pathway. Conclusion: Fenofibrate could potentially prevent PIPN development via the regulation of PPAR-α expression through the reduction in neuroinflammation.
Avraham et al., 2021 (13)	To investigate the role of PPAR-α activity downstream of fatty acid synthase in SGCs on nerve repair.	Fenofibrate (0.2%) was administered as chow pellets for 2 weeks.	SGCs activate PPAR-α signaling to promote axon regeneration in adult peripheral nerves. Conclusion: Fenofibrate improves axon regeneration in adult peripheral nerves via the activation of PPAR-α receptors in the SGCs of dorsal root ganglia.
Othman et al., 2015 (70)	To investigate whether plasma TG level affects the level of 1-deoxySL, which is neurotoxic.	Fenofibrate (160 mg/day) was given to patients with dyslipidemia for 6 weeks.	Fenofibrate specifically lowers 1-deoxySL, which is neurotoxic and elevated in both hereditary sensory neuropathy type 1 and type 2 diabetes. A reduction in 1-deoxySLs is associated with an improvement in nerve conduction velocity. Conclusion: Fenofibrate may have a role in the prevention of diabetic neuropathy by lowering 1-deoxySLs in the plasma of patients with dyslipidemia.
Cho et al., 2014 (14)	To investigate the effect of fenofibrate on diabetic peripheral neuropathy.	Fenofibrate was given to *db/db* mice in combination with antifit-1hexamer and antiflk-1 heptameter (VEGFR inhibition) for 12 weeks.	To ameliorate neural and endothelial damage by activating the PPAR-α-AMPK-PGC-1α-eNOS pathway in *db/db* mice, human umbilical vein endothelial cells, and human Schwann cells. Conclusion: Fenofibrate may have a role in the prevention of neural vascular insufficiency by protecting endothelial cells

Continued on p. 944

Table 7—Continued

Source	Study aims	Treatment	Proposed mechanisms and conclusion
			through the activation of PPAR-α-AMPK-PGC-1α-eNOS pathway.
Retinal neurodegeneration			
Bogdanov et al., 2015 (71)	To evaluate the effects of fenofibric acid, the active metabolite of fenofibrate, in the prevention of retinal neurodegeneration in type 2 diabetes.	Fenofibrate (100 mg/kg/day) was given to *db/db* mice for 1 week.	Prevented the downregulation of glutamate/aspartate transporter induced by diabetes and resulted in a significant decrease in both glial activation and the rate of apoptosis in the ganglion cell layer.

1-deoxySL, 1-deoxysphingolipid; BDNF, brain-derived neurotrophic factor; GDNF, glial-derived neurotrophic factor; eNOS, endothelial nitric oxide synthase; PGC-1α, peroxisome proliferator–activated receptor γ coactivator 1α; PIPN, paclitaxel-induced peripheral neuropathy; SGC, satellite glial cell; VEGFR, vascular endothelial growth factor receptor.

(66) and signaling of neurotrophic receptors (67), respectively. Both proteins are involved in the neurotrophin and MAPK signaling pathways, which were found to be upregulated in our GSEA. SMAD1, which is critical for axon generation (28), was found to be significantly increased after treatment. On the other hand, we found LMNB1 levels to be significantly downregulated after treatment. Increased expression of LMNB1 has been reported to cause central myelin breakdown and demyelinating neuropathy (68).

The current study has several limitations. First, the changes in the age-matched control cohort were not evaluated, but one would expect few changes in the parameters of interest in healthy individuals. Second, a longer end point duration could be considered and will be included in our future studies. Furthermore, we did not see significant differences in other nerve parameters, despite a trend of improvement. This could be explained by CNFD being chosen as the primary outcome for the sample size calculation, but it should be noted that CNFD is the most reliable parameter measured and is the most important clinical indicator for nerve regeneration (69). Moreover, the nerve parameters could have been underestimated when analyzed by an automated software, especially in low-denervated corneas, such as diabetic corneas (69). The newly regenerated corneal nerve fibers are relatively short and fine, making nerve parameters like CNFL less sensitive to be detected. Finally, although we reported alterations in several tear proteins and pathways following fenofibrate treatment, additional mechanistic studies are required to confirm the causal relationship between these pathways and the improved clinical phenotype.

In conclusion, with comprehensive investigation comprising clinical ocular surface assessment and corneal nerve and epithelial cell imaging analysis, we demonstrated that fenofibrate improves ocular surface integrity in diabetic corneas. In addition, detailed ocular surface proteomics suggest that neurotrophic reaction, lipid modulation, and anti-inflammatory and anticoagulation response may contribute to the neuroprotective effects of fenofibrate. Our data support the further evaluation of fenofibrate as a potential novel treatment for DCN.

Acknowledgments. The authors thank colleagues Chen Qi Fan and Vieon Wu Ai Ni from the Department of Endocrinology, Singapore General Hospital, who coordinated and helped with the clinical trial.

Funding. This study was supported by Singapore National Medical Research Council grants MOH-CSAINV21jun-0001 and NMRC/OFLCG/001/2017.

Duality of Interest. No potential conflicts of interest relevant to this article were reported.

Author Contributions. C.H.Y.T. contributed to the manuscript writing, formal analysis, data curation, and visualization. M.T.-Y.L. and I.X.Y.L. performed the laboratory experiments and data curation. S.-K.K. performed the laboratory experiments. L.Z., D.S.G., H.C., and H.W.L.K. contributed to the formal analysis and visualization. A.Y.R.L. contributed to the acquisition of data. P.S.L. contributed to the methodology. J.S.M. and J.-P.K. reviewed the manuscript. T.M.C. contributed to the funding acquisition. H.C.T. contributed to the conceptualization, methodology, formal analysis, manuscript review, and supervision. Y.-C.L. contributed to the conceptualization, methodology, investigation, formal analysis, manuscript review, supervision, and funding acquisition. H.C.T. and Y.-C.L. is the guarantor of this work and, as such, had full access to all the data in the study and takes responsibility for the integrity of the data and the accuracy of the data analysis.

Prior Presentation. Parts of this study were presented orally at the Association for Research in Vision and Ophthalmology Annual Meeting, Denver, CO, 1–4 May 2022; in poster form at the 32nd International Congress of Medical Women International Association, Taipei, Taiwan, 24–26 June 2022; and orally at Wong Hock Boon Society Research Day, National University of Singapore, Singapore, 29 January 2022.

References

1. Iqbal Z, Azmi S, Yadav R, et al. Diabetic peripheral neuropathy: epidemiology, diagnosis, and pharmacotherapy. Clin Ther 2018;40:828–849

2. Zhou T, Lee A, Lo ACY, Kwok JSWJ. Diabetic corneal neuropathy: pathogenic mechanisms and therapeutic strategies. Front Pharmacol 2022;13:816062

3. Bodman MA, Varacallo M. Peripheral Diabetic Neuropathy. Treasure Island, FL, StatPearls Publishing, 2022
4. Labetoulle M, Baudouin C, Calonge M, et al. Role of corneal nerves in ocular surface homeostasis and disease. Acta Ophthalmol 2019;97:137–145
5. Al-Aqaba MA, Dhillon VK, Mohammed I, Said DG, Dua HS. Corneal nerves in health and disease. Prog Retin Eye Res 2019;73:100762
6. Mansoor H, Tan HC, Lin MTY, Mehta JS, Liu YC. Diabetic corneal neuropathy. J Clin Med 2020;9:1–24
7. Mastropasqua L, Lanzini M, Dua HS, et al. In vivo evaluation of corneal nerves and epithelial healing after treatment with recombinant nerve growth factor for neurotrophic keratopathy. Am J Ophthalmol 2020;217:278–286
8. Han L, Shen WJ, Bittner S, Kraemer FB, Azhar S. PPARs: regulators of metabolism and as therapeutic targets in cardiovascular disease. Part II: PPAR-β/δ and PPAR-γ. Future Cardiol 2017;13:279–296
9. Poulsen LI, Siersbæk M, Mandrup S. PPARs: fatty acid sensors controlling metabolism. Semin Cell Dev Biol 2012;23:631–639
10. Balfour JA, McTavish D, Heel RC. Fenofibrate. A review of its pharmacodynamic and pharmacokinetic properties and therapeutic use in dyslipidaemia. Drugs 1990;40:260–290
11. Wiggin TD, Sullivan KA, Pop-Busui R, Amato A, Sima AAF, Feldman EL. Elevated triglycerides correlate with progression of diabetic neuropathy. Diabetes 2009;58:1634–1640
12. Caillaud M, Patel NH, White A, et al. Targeting peroxisome proliferator-activated receptor-α (PPAR-α) to reduce paclitaxel-induced peripheral neuropathy. Brain Behav Immun 2021;93:172–185
13. Avraham O, Feng R, Ewan EE, Rustenhoven J, Zhao G, Cavalli V. Profiling sensory neuron microenvironment after peripheral and central axon injury reveals key pathways for neural repair. eLife 2021;10:1–30
14. Cho YR, Lim JH, Kim MY, et al. Therapeutic effects of fenofibrate on diabetic peripheral neuropathy by improving endothelial and neural survival in db/db mice. PLoS One 2014;9:e83204
15. Keech A, Simes RJ, Barter P, et al.; FIELD Study Investigators. Effects of long-term fenofibrate therapy on cardiovascular events in 9795 people with type 2 diabetes mellitus (the FIELD study): randomised controlled trial. Lancet 2005;366:1849–1861
16. Matlock HG, Qiu F, Malechka V, et al. Pathogenic role of PPARα downregulation in corneal nerve degeneration and impaired corneal sensitivity in diabetes. Diabetes 2020;69:1279–1291
17. Liu YC, Jung ASJ, Chin JY, Yang LWY, Mehta JS. Cross-sectional study on corneal denervation in contralateral eyes following SMILE versus LASIK. J Refract Surg 2020;36:653–660
18. Liu YC, Lin MT, Mehta JS. Analysis of corneal nerve plexus in corneal confocal microscopy images. Neural Regen Res 2021;16:690–691
19. Chen X, Graham J, Petropoulos IN, et al. Corneal nerve fractal dimension: a novel corneal nerve metric for the diagnosis of diabetic sensorimotor polyneuropathy. Invest Ophthalmol Vis Sci 2018;59:1113–1118
20. Sindt CW, Lay B, Bouchard H, Kern JR. Rapid image evaluation system for corneal in vivo confocal microscopy. Cornea 2013;32:460–465
21. Yawata N, Selva KJ, Liu Y-C, et al. Dynamic change in natural killer cell type in the human ocular mucosa in situ as means of immune evasion by adenovirus infection. Mucosal Immunol 2016;9:159–170
22. Teo CHY, Ong HS, Liu Y-C, Tong L. Meibomian gland dysfunction is the primary determinant of dry eye symptoms: Analysis of 2346 patients. Ocul Surf 2020;18:604–612
23. Bron AJ, Evans VE, Smith JA. Grading of corneal and conjunctival staining in the context of other dry eye tests. Cornea 2003;22:640–650
24. Chin JY, Lin MT-Y, Lee IXY, Mehta JS, Liu Y-C. Tear neuromediator and corneal denervation following SMILE. J Refract Surg 2021;37:516–523
25. Liu Y-C, Yam GH-F, Lin MT-Y, et al. Comparison of tear proteomic and neuromediator profiles changes between small incision lenticule extraction (SMILE) and femtosecond laser-assisted in-situ keratomileusis (LASIK). J Adv Res 2020;29:67–81
26. Teo G, Kim S, Tsou C-C, et al. mapDIA: preprocessing and statistical analysis of quantitative proteomics data from data independent acquisition mass spectrometry. J Proteomics 2015;129:108–120
27. Subramanian A, Tamayo P, Mootha VK, et al. Gene set enrichment analysis: a knowledge-based approach for interpreting genome-wide expression profiles. Proc Natl Acad Sci U S A 2005;102:15545–15550
28. Ueberham U, Arendt T. The role of Smad proteins for development, differentiation and dedifferentiation of neurons. In Trends in Cell Signaling Pathways in Neuronal Fate Decision. Wislet-Gendebien S, Ed. Rijeka, Croatia, IntechOpen, 2013, pp. 75–112
29. Chicherin IV, Dashinimaev E, Baleva M, Krasheninnikov I, Levitskii S, Kamenski P. Cytochrome *c* oxidase on the crossroads of transcriptional regulation and bioenergetics. Front Physiol 2019;10:644
30. Chao C, Wang R, Jones M, et al. The relationship between corneal nerve density and hemoglobin A1c in patients with prediabetes and type 2 diabetes. Invest Ophthalmol Vis Sci 2020;61:26
31. Zhang J, Dai Y, Wei C, Zhao X, Zhou Q, Xie L. DNase I improves corneal epithelial and nerve regeneration in diabetic mice. J Cell Mol Med 2020;24:4547–4556
32. Mocan MC, Durukan I, Irkec M, Orhan M. Morphologic alterations of both the stromal and subbasal nerves in the corneas of patients with diabetes. Cornea 2006;25:769–773
33. So WZ, Wong NSQ, Tan HC, et al. Diabetic corneal neuropathy as a surrogate marker for diabetic peripheral neuropathy. Neural Regen Res 2022;17:2172–2178
34. Beuerman RW, Schimmelpfennig B. Sensory denervation of the rabbit cornea affects epithelial properties. Exp Neurol 1980;69:196–201
35. Jiang Q-W, Kaili D, Freeman J, et al. Diabetes inhibits corneal epithelial cell migration and tight junction formation in mice and human via increasing ROS and impairing Akt signaling. Acta Pharmacol Sin 2019;40:1205–1211
36. Di G, Qi X, Zhao X, Zhang S, Danielson P, Zhou Q. Corneal epithelium-derived neurotrophic factors promote nerve regeneration. Invest Ophthalmol Vis Sci 2017;58:4695–4702
37. Tavakoli M, Kallinikos PA, Efron N, Boulton AJM, Malik RA. Corneal sensitivity is reduced and relates to the severity of neuropathy in patients with diabetes. Diabetes Care 2007;30:1895–1897
38. Gao Y, Zhang Y, Ru Y-S, et al. Ocular surface changes in type II diabetic patients with proliferative diabetic retinopathy. Int J Ophthalmol 2015;8:358–364
39. Dartt DA. Neural regulation of lacrimal gland secretory processes: relevance in dry eye diseases. Prog Retin Eye Res 2009;28:155–177
40. Serin D, Karsloğlu S, Kyan A, Alagöz G. A simple approach to the repeatability of the Schirmer test without anesthesia: eyes open or closed? Cornea 2007;26:903–906
41. Yang L, Di G, Qi X, et al. Substance P promotes diabetic corneal epithelial wound healing through molecular mechanisms mediated via the neurokinin-1 receptor. Diabetes 2014;63:4262–4274
42. Tummanapalli SS, Willcox MDP, Issar T, et al. Tear film substance P: a potential biomarker for diabetic peripheral neuropathy. Ocul Surf 2019;17:690–698
43. Markoulli M, You J, Kim J, et al. Corneal nerve morphology and tear film substance p in diabetes. Optom Vis Sci 2017;94:726–731
44. Kim HC, Cho YJ, Ahn CW, et al. Nerve growth factor and expression of its receptors in patients with diabetic neuropathy. Diabet Med 2009;26:1228–1234
45. Terenghi G, Mann D, Kopelman PG, Anand P. trkA and trkC expression is increased in human diabetic skin. Neurosci Lett 1997;228:33–36
46. Rodríguez-Peña A, Botana M, González M, Requejo F. Expression of neurotrophins and their receptors in sciatic nerve of experimentally diabetic rats. Neurosci Lett 1995;200:37–40
47. Tang M, Luo M, Lu W, et al. Nerve growth factor is closely related to glucose metabolism, insulin sensitivity and insulin secretion in the second trimester: a case-control study in Chinese. Nutr Metab (Lond) 2020;17:98

48. Müller LJ, Marfurt CF, Kruse F, Tervo TMT. Corneal nerves: structure, contents and function. Exp Eye Res 2003;76:521–542
49. Yang LWY, Mehta JS, Liu Y-C. Corneal neuromediator profiles following laser refractive surgery. Neural Regen Res 2021;16:2177–2183
50. Agthong S, Kaewsema A, Tanomsridejchai N, Chentanez V. Activation of MAPK ERK in peripheral nerve after injury. BMC Neurosci 2006;7:45
51. Brownlee M, Aiello LP, Cooper ME, Vinik AI, Plutzky J, Boulton AJM. Chapter 33 - complications of diabetes mellitus. In Williams Textbook of Endocrinology (Thirteenth Edition). Melmed S, Polonsky KS, Larsen PR, Kronenberg HM, Eds. Philadelphia, Elsevier; 2016, pp. 1484–1581
52. Verheijen MHG, Peviani M, Hendricusdottir R, et al. Increased axonal ribosome numbers is an early event in the pathogenesis of amyotrophic lateral sclerosis. PLoS One 2014;9:e87255
53. Tavakoli M, Marshall A, Pitceathly R, et al. Corneal confocal microscopy: a novel means to detect nerve fibre damage in idiopathic small fibre neuropathy. Exp Neurol 2010;223:245–250
54. Iqbal Z, Bashir B, Ferdousi M, et al. Lipids and peripheral neuropathy. Curr Opin Lipidol 2021;32:249–257
55. Nakano Y, Arima T, Tobita Y, Uchiyama M, Shimizu A, Takahashi H. Combination of peroxisome proliferator-activated receptor (Ppar) alpha and gamma agonists prevents corneal inflammation and neovascularization in a rat alkali burn model. Int J Mol Sci 2020;21:1–16
56. Koo JW, Russo SJ, Ferguson D, Nestler EJ, Duman RS. Nuclear factor-kappaB is a critical mediator of stress-impaired neurogenesis and depressive behavior. Proc Natl Acad Sci U S A 2010;107:2669–2674
57. Levenson JM, Choi S, Lee S-Y, et al. A bioinformatics analysis of memory consolidation reveals involvement of the transcription factor c-rel. J Neurosci 2004;24:3933–3943
58. Gutierrez H, Davies AM. Regulation of neural process growth, elaboration and structural plasticity by NF-κB. Trends Neurosci 2011;34:316–325
59. Nasirikenari M, Segal BH, Ostberg JR, Urbasic A, Lau JT. Altered granulopoietic profile and exaggerated acute neutrophilic inflammation in mice with targeted deficiency in the sialyltransferase ST6Gal I. Blood 2006;108:3397–3405
60. Qian Y, Zeng Y, Lin Q, et al. Association of platelet count and plateletcrit with nerve conduction function and peripheral neuropathy in patients with type 2 diabetes mellitus. J Diabetes Investig 2021;12:1835–1844
61. Bellei E, Vilella A, Monari E, et al. Serum protein changes in a rat model of chronic pain show a correlation between animal and humans. Sci Rep 2017;7:41723
62. Leppin K, Behrendt A-K, Reichard M, et al. Diabetes mellitus leads to accumulation of dendritic cells and nerve fiber damage of the subbasal nerve plexus in the cornea. Invest Ophthalmol Vis Sci 2014;55:3603–3615
63. Yassine HN, Trenchevska O, He H, et al. Serum amyloid a truncations in type 2 diabetes mellitus. PLoS One 2015;10:e0115320
64. Mooyaart AL, Valk EJJ, van Es LA, et al. Genetic associations in diabetic nephropathy: a meta-analysis. Diabetologia 2011;54:544–553
65. Jiao Y, Jiang S, Wang Y, et al. Activation of complement C1q and C3 in glomeruli might accelerate the progression of diabetic nephropathy: evidence from transcriptomic data and renal histopathology. J Diabetes Investig 2022;13:839–849
66. Guan L, Yu WS, Shrestha S, et al. TTC9A deficiency induces estradiol-mediated changes in hippocampus and amygdala neuroplasticity-related gene expressions in female mice. Brain Res Bull 2020;157:162–168
67. Bucci C, Alifano P, Cogli L. The role of rab proteins in neuronal cells and in the trafficking of neurotrophin receptors. Membranes (Basel) 2014;4:642–677
68. Hutchison CJ. B-type lamins in health and disease. Semin Cell Dev Biol 2014;29:158–163
69. Chin JY, Yang LWY, Ji AJS, et al. Validation of the use of automated and manual quantitative analysis of corneal nerve plexus following refractive surgery. Diagnostics (Basel) 2020;10:E493
70. Othman A, Benghozi R, Alecu I, et al. Fenofibrate lowers atypical sphingolipids in plasma of dyslipidemic patients: a novel approach for treating diabetic neuropathy? J Clin Lipidol 2015;9:568–575
71. Bogdanov P, Hernández C, Corraliza L, Carvalho AR, Simó R. Effect of fenofibrate on retinal neurodegeneration in an experimental model of type 2 diabetes. Acta Diabetol 2015;52:113–122